Proceedings of the VI Brazilian Conference on Neural Networks - VI Congresso Brasileiro de Redes Neurais
pp. 115–120, June 2–5, 2001 - Centro Universitario da FEI, Sao Paulo - SP - Brazil

Topological Rings for Neural Network Preprocessing in Calorimetry

Denis O. Damazio[1], José M. Seixas[1]
[1] Laboratório de Processamento de Sinais (LPS)
COPPE/EE/UFRJ, CP 68504, Rio de Janeiro 21945-970, Brazil
E-mails: Denis.Oliveira.Damazio@cern.ch, seixas@lps.ufrj.br

Abstract

The next experiments in high energy physics depends a lot on good calorimeter (energy meters) data. During experimental beam tests for a calorimeter calibration at CERN, the European Institute for Particle Physics, contaminations on the beam line can arise as great difficult to the calibration procedure. This work presents a neural network system to identify these contaminations using a preprocessing based on the particles deposition profiles. Comparisons with other analysis methodologies shows an efficiency greater than 93.5% in data and contamination identification.

1. Introduction

During the last century, many experiments were assembled to search deeper the rules that govern the Universe. In the present days, science has been promoting collaborative work among research institutes, to build huge and very expensive experiments in many fields. This cooperative structure increases the exchange of ideas and distributes costs between its members. Without this cost distribution, many experiments could never be feasible.

One of such collaborative efforts in high energy physics has been powering the European Laboratory for Particle Physics (CERN) [1], which is dedicated to the study of elementary physics. Many European countries collaborate to perform the experiments that can prove or reject new theories in the field. CERN is located in the franc-swiss boarder and is now building a new particle accelerator, the Large Hadron Collider (LHC).

The LHC comprises a 27 Km tunnel, which is hundred meters under the floor. This accelerator, built with superconductive techniques will be able, when operational by the year 2007, to increase the particles energy up to 14 TeV (Tera-electron-Volts) in the center of mass, an energy level never reached by this kind of experiment. To analise the products of the collisions, two large detectors are also being constructed, the CMS and the ATLAS.

The ATLAS (A Toroidal Lhc ApparatuS) [2] is shown in Figure 1. Particles from LHC should come in both senses through the central detector axis, colliding in the central point. The products of these collisions should hit the detector from the center to its outside, passing thought many sub-detectors. The first sub-detector is the Inner

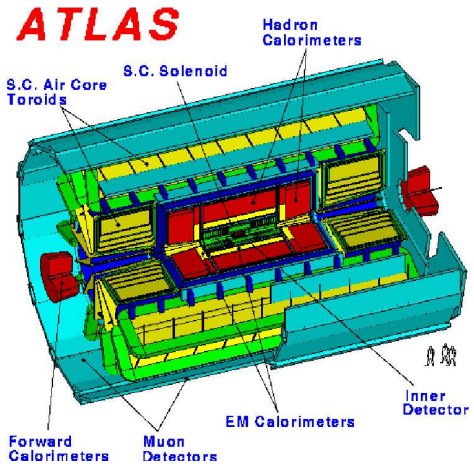

Figure 1: The ATLAS detector and all its sub-detectors. See text for details.

Detector, responsible for tracking estimation of the incoming particles. After that, the Electromagnetic and the Hadronic Calorimeters will measure the particle energy. A special detector to track important particles (muons) for the expected physics at LHC completes the ATLAS detector. Two solenoids are responsible for creating huge magnetic fields to help in particle charge detection.

Presently, many sub-detectors are in final production phase and beginning to be calibrated with experimental particle beam produced by a smaller particle accelerator. The calibration procedure consists of studying the response of the detectors and how to convert the electronics signals into meaningful variables. One of the detectors being calibrated by now is the hadronic calorimeter.

Although the beam quality is very high for the calibration procedure, it is impossible to avoid the creation of particles that behave as contaminating particles for the particle beam selected. So, some discriminating procedure must be used to provide a calibration free of such outsider particles. Our approach is to use neural networks to perform automatic particle discrimination detecting the outsider particles and obtaining a purified data set for calibration.

In this work, particle discrimination is developed by using a topological preprocessing schema on the information provided by this hadronic calorimeter of ATLAS. Such topological approach allows to reduce the dimension of data input space, which is high due to the detector

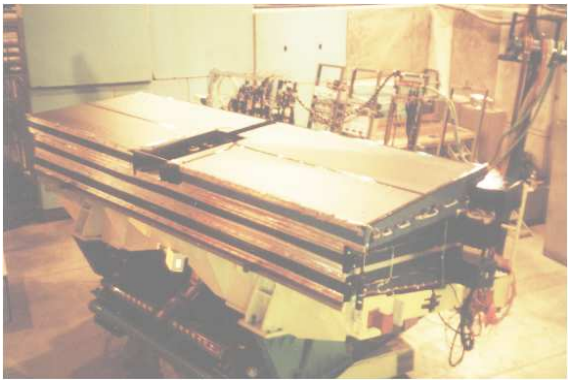

Figure 2: Two calorimeter modules during calibration beam tests.

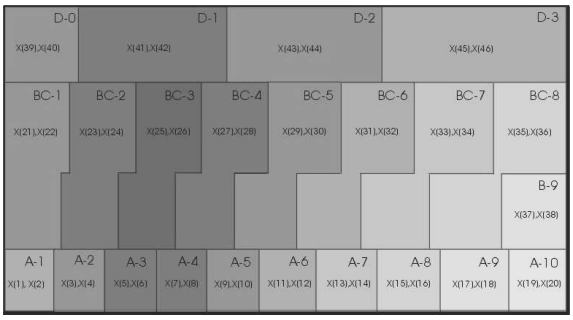

Figure 3: Detector cells in one module of the TileCal detector.

granularity. Thus, the classification task may be made easier and faster.

The next section describes the calorimeter and its properties. The third section shows the first results and comparisons with classical methodologies used by physicists. Conclusions are derived in the fourth section.

2. Calorimetry

The ATLAS Hadron Calorimeter will form a toroid around the collision point, receiving the incoming particles into its inner part and measuring their energy. In order to facilitate the assembling and transport procedures, the calorimeter was divided into 64 modules each one comprising $1/64$ of the toroid. This modules are now in calibration phase. Figure 2 shows two lateral sections of the calorimeter being prepared for a testbeam on a mechanical table.

The detection principle is quite simple. The calorimeter is made of iron plates placed between a active (plastic) material [3]. The iron absorbs most of the incoming particle energy. Typically, the particles, when colliding in the calorimeter mass, lose part of their energy and produce many other particles. These ones will repeat the same process until all the energy of the first particle is completely dispersed into the calorimeter structure. The energy dispersed can be partially collected by the active material which produces light by scintillation. This light is proportional to the energy quantity let in the detector. Using a net of optical fibers this light is taken to the electronic read-out of the detector. Since the active material lay like tiles in a roof in the detector module structure, the ATLAS hadronic calorimeter is called Tile Calorimeter, or simply TileCal.

Fibers coming from the same areas on the module surface are grouped together, defining cell regions in the detector. Figure 3, shows the cell disposition for half a module of TileCal (each half is tested separately).

The 23 cells are organized in three layers in deep. The first is composed of 10 rectangular cells, the second comprises 9 irregular shaped cells, and the third has 4 larger rectangular cells.

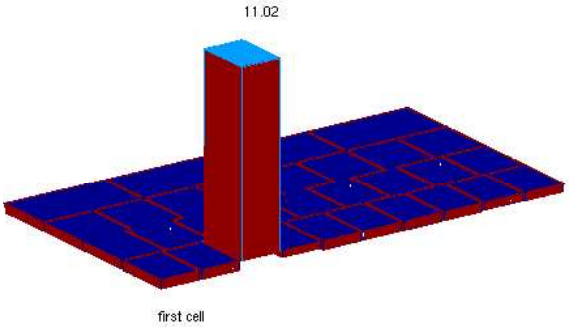

Figure 4: Electron deposition profile in a TileCal module. Almost all the energy is contained in the first cell touched by the particle.

Each particle has a different energy deposition profile on the detector cells, depending on its intrinsic interaction properties [4]. So, it is possible to detect the particle type only by studying its deposition profiles.

For instance, one of the particles used during the calibration tests is the electron. This particle deposits most of its energy (more than 60%) in the first calorimeter cell it touches. We can see an example of a electron interaction in the Figure 4. This was produced by a beam set to 20 GeV (Giga-electron-Volts). Most of the energy (more that 11 GeV), is contained in the first calorimeter cell touched, in the present case, the third cell of the first layer.

Another particle type used in calibration tests is the pion. This particle does not interact with the first mass portion it encounters as electrons do. Their interaction typically begins at the end of the first cell, spreading a great quantity of energy around the interaction point. The Figure 5 brings an event of pion interaction. As can be seen, Just a small quantity of energy was deposited in the first cell touched (the same of the electron event). Most of the energy was deposited in the second cell. Also, it should be noted that the energy peak (5.63 GeV) is

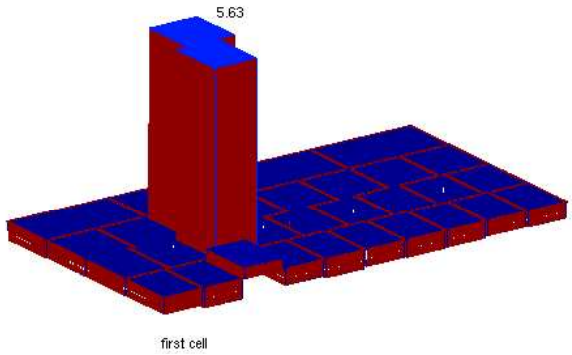

Figure 5: Pion deposition profile in a TileCal module. The major part of the energy is contained in the cell of the second lay hit by the particle.

smaller than that of the electron event (11.02 GeV). This is caused by the larger energy spread in the pion case, that reduces the maximum energy concentration.

These two profiles are based in the presence of a central tower with greater energy level and cells around this maximum with less energy. So, in the electron event, the tower in the first layer accounts for the maximum. A ring (open) with less energy can be defined with the cells around this maximum point. The same can be done with the pion event deposition profile, but, clearly, the proportion of energy between these rings of cells is not the same. For electrons, the center predominates over the ring, while for pions, the energy in the rings is more distributed. This fact will be further used when we discuss our preprocessing technique.

A third particle type, muons, lets just a very small energy in the detector, forming a track along all the calorimeter deep, from the cell in the first layer until the cell in the last layer [5].

So, as can be noted, the problem of particle detection is a pattern recognition problem. This is the reason the approach based in neural networks was followed.

During the beam tests, the three types of particles already discussed, electrons, pions and muons, are used. Unfortunately, contamination events appear in the beam line. Pion data sets are contaminated by muon events (up to 30%) and the electron set have both pion (30 %, but up to 45 % has been detected) and muon (2-25 %) contaminating events. The muon set is the only one that can be considered a pure data set. Neural networks are then applied to this sets to identify this cross contaminations.

3. Results

The neural network is simulated using the Fortran JetNet-2.0 package [6]. This package can simulate the network and perform a training on its weights based on the backpropagation method. This is supervised method

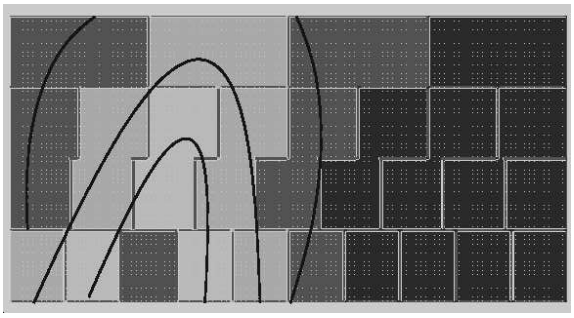

Figure 6: Electron deposition profile based on ring structure.

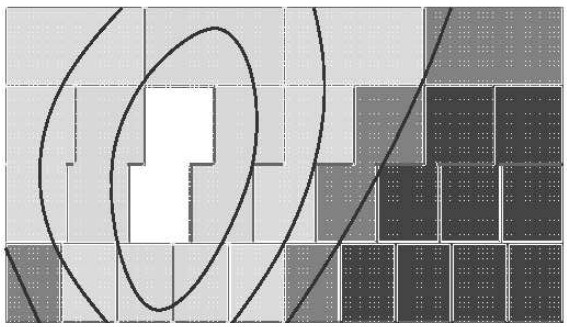

Figure 7: Pion deposition profile based ring structure.

[7], which depends, for the training phase, on the definition of input-output pairs. This is a problem, since, with the contaminations, not all the events in each data set are really from the particle type of that data set. For instance, contaminating muons in a pion sample will be considered as pions when defining the outputs to be used for that data sample during the neural network training. As we will see, this will not be a problem, since the network will be able to extract from the data sets the features that define the different sets, being able to identify the contaminations from the pure events.

In order to profit from the differences in the particles deposition profile, two ring structures were defined with the calorimeter cells as inputs to the neural network. One was based in the electrons deposition profile and the other in the pions deposition profile. The initial idea was to optimize the detection of each kind of particle by using a preprocessing based on the deposition profile of that particle type. For the electron deposition profile-like rings, Figure 6 brings the cells selection for each ring.

The first ring is the main interaction point. In the present case, this is the third cell of the first layer. A ring composed of all the cells around this point was defined reaching until the second layer. A third ring reaching the third layer also appears and the last ring used has 2 cells at the left and three at the right of the first three rings. The lines in the figure, help to show the second, third and fourth rings. Some cells at the right of the module do not receive any signal (since the beam was not targeting this part of the detector), and, so, are not included in the rings.

The Figure 7 shows the same situation when the pion deposition profile-like rings are assembled with the calorimeter cells. Now, the first ring is the cell in the second layer, while the other rings are assembled around it. The third and fourth rings are open rings.

Using such preprocessing, by inputing the sum of the cells in a ring instead of the each cell separately to the neural network, a reduction on the input space dimension from 23 to 4 is obtained. Clearly, this can have a large impact in the system speed, what may be helpful when considering online applications [8].

The data sets, acquired in the 1999 testbeam, were splitted into training and testing sets. This helps to evaluate the system performance when events never used to train the network are concerned. The network was composed of 4 input nodes, 8 nodes in the hidden layer and 3 output nodes, each one assigned to one particle type. During the training phase, the output related to the set of the incoming event was set to one, while the two others were set to minus one. So, an electron event, or even a contaminating pion or muon event on the electron set, would receive a +1 electron output, while the others would be set to -1. In the testing phase maximum probability (output value) was used as decision factor.

The inputs were normalized in order to couple with the small linear range of the activation functions of the network neurons (hyperbolic tangent). The normalization was performed by dividing each of the four input variables by the square root of the absolute value of their sum. This was done to keep some energy information, helping to discriminate muon events on the data sets.

The two neural networks (one for the electron rings and the other for the pion rings) were trained with 120 thousand training steps with data coming from a 100 GeV experiment and its three outputs for the three data sets can be viewed in the Figure 8.

These outputs are for the pion rings used as inputs. Only test data sets are considered here. Each column brings a histogram of one of the outputs in the three data sets (each of the lines). So, for instance, the first top left histogram is the electron output for the electron set events. The histogram at the right of this first one is the pion output in the same set. It should be expected that only the histogram on the main diagonal of this histogram matrix should have events with value +1. But events with negative values appear in the electron output to the electron set. Also, events with positive values of the pion output to the electron set can be found. It seems that pion events are being found in the electron data set. In fact, the neural network may be identifying the contaminating pions in the data sample.

We need to check that information, and for that, energy cuts can be used [9]. Variables such as the fraction of energy deposited in the first layer of cells, in the third layer, total energy or auxiliary detectors information can be used to establish an offline and energy depend methodology for discriminating the particles. One example of comparison between both methods can be found in the

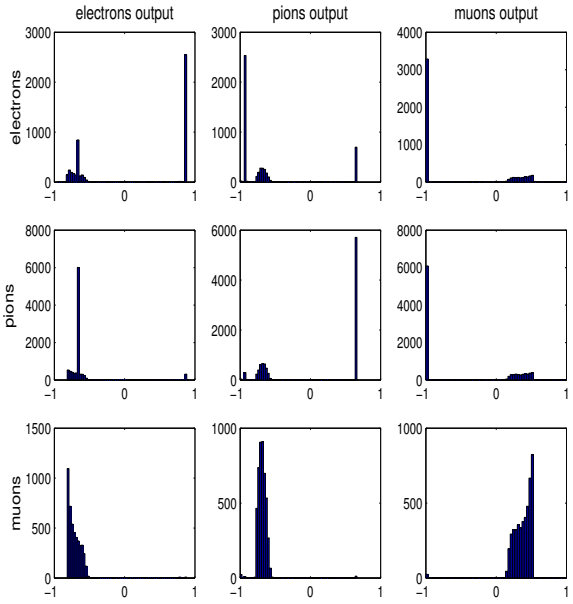

Figure 8: Network outputs (columns) for the three test data sets (rows).

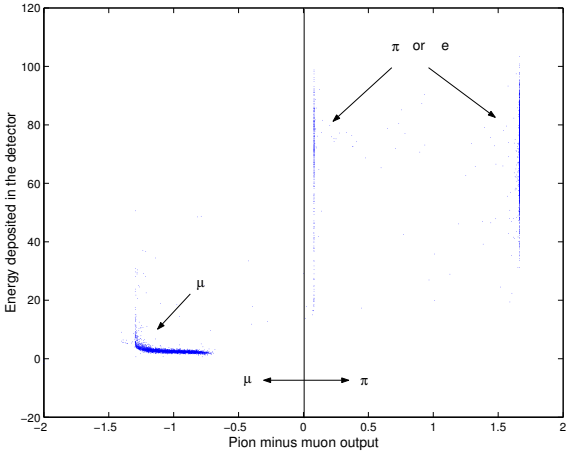

Figure 9: Pion minus muon neural network output versus the total energy in the module.

E	e	π	μ	tot
20	93.23%	90.33%	97.82%	93.74%
100	96.13%	97.50%	99.53%	97.71%
180	96.68%	90.77%	99.53%	95.59%

E	e	π	μ	tot
20	92.22%	89.20%	98.04%	93.08%
100	93.42%	95.43%	98.66%	95.81%
180	95.06%	93.60%	99.05%	95.88%

Table 1: Comparison table for the three data sets in three energy levels. The first table refers to the network with electron deposition profile-like rings, the second to the pion deposition profile-like rings.

Figure 9. In this figure, the neural network pion minus muon output (factor for discriminating possible muons in the pion set), is compared with the total energy in the calorimeter for the pion test set. The events in the positive side of the horizontal axis, are those considered by the neural network as being real pions. These are the same events with a higher energy level (as indicated in the vertical axis). On the other hand, the events in the negative side on the horizontal axis (considered as muons by the neural network) were the same that deposited less energy in the detector, what is a physical characteristic of the muon interaction.

Using a set of cuts based on physical properties of the beam interaction, we composed a complete benchmark methodology. This methodology has to be adjusted for each energy range, what is not necessary for the neural network procedure, that automatically adjust itself to the new conditions. Comparing for each set the identification of both, pure particles and contaminations for three different energy levels, we have the results expressed in the Table 1. The first table refers to the electron profile-like rings and the second based to the pion profile-like rings preprocessing. The three energy levels selected represent three important energy ranges, 20 GeV (low energy), 100 GeV (medium range) and 180 GeV (high energy).

So, for example, in the electron set at 20 GeV, 59% of the events were considered by both methodologies (energy cuts and neural network) as being real electrons, 32.14% as being contaminating pions and, finally, 2.09% as being contaminating muons. In total, as shown in the table, 93.23% of the events received the same votes by both methods. The important values of total agreement (never smaller than 93%) shows that the neural network methodology agrees with the physical concept of interactions in TileCal.

As can be seen, both preprocessing methods obtained an smaller agreement for pions at 20 GeV. This is possible due to the fact that pion interactions at 20 GeV, a very low energy level, do not develop too far from the beginning of the calorimeter. The lower energy particle can not penetrate much in the calorimeter structure and begin to produce interactions very similar to the electron ones, being easily confused with this second particle type.

E	e	π	μ	tot
20	93.62%	93.52%	98.10%	95.06%
100	95.73%	95.91%	99.39%	97.00%
180	96.46%	91.60%	99.33%	95.74%

Table 2: Comparison results when both ring structures are used for preprocessing.

agreem.	elec.	pion	muon	tot.
gran.	95.30%	94.37%	99.50%	96.39%
rings	95.73%	95.91%	99.39%	97.00%

Table 3: Comparison of the agreement levels for using the two ring structures or full calorimeter granularity as inputs to the neural network (100 GeV).

So, the electron profile-like rings can label many pions as being electrons, and the pion profile-like rings do not seem to have enough granularity to correctly separate electrons from pions. This leads to the idea of trying to balance both procedures, profiting from the best characteristics of both methods. In order to leave the decision to the neural network, both procedures were used at the same time. A network with 8 input nodes (4 for each ring set) was trained for the same three energy levels studied before. The results are expressed in the Table 2.

As can be noted when comparing this agreement table with the two previous ones, the 20 GeV case profited a lot from the two ring structures preprocessing. Every agreement result was increased in this energy, with a special prominence to the pion set result, which increased more than 3%.

So, it was possible to reduce the initial dimensionality from 23 to only 8, assuring a high level confidence in the result, and keeping the automatism of the neural network methodology, which does not depend, as the energy cut method, on a specialist pre-analysis.

Finally, we can compare for the 100 GeV case, the performance of the system with the proposed preprocessing and a neural network system with the 23 input nodes (one for each cell). The results are shown in the Table 3. As can clearly be seen, just a small reduction on the muon agreement (0.11%) can be accounted. For the pion set a gain of more than 1.5% was obtained by the new technique. In the overall result the two ring structures had a better performance.

4. Conclusions

A preprocessing for a neural network application in the high energy physics was obtained. Two different ring structures were studied and the results benchmarked against classical procedures showed a good agreement with the problem physics. In order to increase the system

performance at low energies (when the deposition profiles of the different particles look similar), an approach using both ring structures was successfully applied.

The benchmark system used is based in a set of energy cuts, which can not be easily automatized. The neural network application, can tune itself during the training, not needing a specialist interference.

The situation studied included an interesting challenge to the neural network trained by the backpropagation supervised method. Since natural data contamination was present, wrong labeling of events during the training phase was unavoidable. The feature extraction capacity of the neural network was able to correctly identify this problem, even when the contamination level was very high (At 180 GeV, only 22% of the electron events were real electron events). The usage of self-organizing methods is part of the future of this application as another possible approach.

The usage of ring structures is quite common in calorimetry applications [10]. The neural network system is independent of the calorimeter being used. The application here developed can, then, be adapted in other calorimetry experiments.

Finally, the dimensionality reduction obtained with the preprocessing studied was very high. From the 23 dimensions initial input space a maximum of 8 were used in our application. This can have a huge impact when trying to apply this technique online. Typically, in this situation, time restriction (both to neural network response time and training time) are strong. The reduction can represent an increase of more than 2 times in the processing speed.

5. *

Acknowledgments We are thankful to the support given to this project by CAPES, CNPq, FAPERJ (Brazil) and CERN (Switzerland). We would also like to thank our colleagues of the TileCal collaboration for the data sets used in this work.

References

[1] CERN. European laboratory for particle physics, 2003. http://www.cern.ch.

[2] ATLAS. A toroidal lhc aparatus, 2003. http://www.cern.ch/Atlas.

[3] ATLAS Collaboration. Tile calorimeter technical design report. Technical Report CERN/LHCC/96-42, CERN, 1996.

[4] R. Wigmans. Advances in hadron calorimetry. *Rev. Nucl. Part. Sci.*, 4:133, 1991.

[5] Z. A. *et al*. Response of the atlas tile calorimeter prototype to muons. *Nucl. Instr. Meth*, A388:64–78, 1997.

[6] L. *et al*. Pattern recognition in high energy physics with artificial neural networks - jetnet 2.0. *Comput. Phys. Comm*, 70:167, 1992.

[7] S. Haykin. *Neural Networks, A Comprehensive Foundation*. Prentice-Hall, 2 edition, 1999.

[8] D. O. Damazio and J. M. Seixas. An online calorimeter trigger for removing outsiders from particle beam calibration tests. In *VIII International Workshop on Advanced Computing and Analysis Techniques in Physics Research*, Moscow, 2002.

[9] J. Seixas and D. Damazio. A neural discriminator capable to identify impurities in the data sample. In *Fifth IEEE International Conference on Electronics, Circuits and Systems*, volume 2, pages 261–264, Lisbon - Portugal, 1998.

[10] P. A. *et al*. Hadronic shower development in iron-scintillator tile calorimetry. *Nucl. Instr. Meth.*, A443:51–70, 2000.